FULL PAPER

Syntheses, structures and solution behaviour of cyclotriphosphato complexes of Pd(II), Pt(II) and Pt(IV)

Sou Kamimura,[a] Shigeki Kuwata,[b] Masakazu Iwasaki[c] and Youichi Ishii *[d]

[a] Institute of Industrial Science, The University of Tokyo, Komaba, Meguro-ku, Tokyo 153-8505, Japan

[b] Department of Applied Chemistry, Graduate School of Science and Engineering, Tokyo Institute of Technology, O-okayama, Meguro-ku, Tokyo 152-8552, Japan

[c] Department of Applied Chemistry, Faculty of Engineering, Saitama Institute of Technology, Okabe, Saitama 369-0293, Japan

[d] Department of Applied Chemistry, Faculty of Science and Engineering, Chuo University, Kasuga, Bunkyo-ku, Tokyo 112-8551, Japan

The cyclotriphosphate ion ($P_3O_9{}^{3-}$) as a PPN [PPN = $(Ph_3P)_2N^+$] salt reacted in CH_2Cl_2 at room temperature with the cationic solvated complexes of Pd(II) and Pt(II), $[M(phosphine)_2(Me_2CO)_2]^{2+}$ [M = Pd, Pt; phosphine = PPh_3, $PMePh_2$, 1/2 $Ph_2P(CH_2)_2PPh_2$ (dppe), 1/2 $Ph_2P(CH_2)_4PPh_2$ (dppb)], to give the anionic P_3O_9 complexes (PPN)-$[Pd(P_3O_9)(PPh_3)_2]$ (1), $(PPN)[Pd(P_3O_9)(PMePh_2)_2]$ (2), $(PPN)[Pt(P_3O_9)(PPh_3)_2]$ (3), $(PPN)[Pt(P_3O_9)(PMePh_2)_2]$ (4), $(PPN)[Pt(P_3O_9)(dppe)]$ (5) and $(PPN)[Pt(P_3O_9)(dppb)]$ (6). Crystallographic studies revealed that the P_3O_9 ligand in complexes 1–4 and 6 adopts a normal chair conformation and behaves as a pseudo-tridentate ligand with two normal M–O bonds and an additional weak M $\cdots$ O interaction. In 1 and 3, the terminal P_3O_9 oxygen atom weakly bound to the metal centre forms relatively strong intramolecular CH $\cdots$ O hydrogen bonds with the phosphine ligands. In contrast, the P_3O_9 ligand in 5 is bidentate and takes a pseudo-boat conformation. Complexes 1–6 are fluxional in solution and exhibit only one singlet due to the P_3O_9 ligand in the $^{31}P-\{^1H\}$ NMR spectra at room temperature; the signals of complexes 4–6 split into two at −40 to −70 °C. The activation parameters for the fluxional behaviour of 6 were determined by the line shape analysis of the variable temperature $^{31}P-\{^1H\}$ NMR spectra. The Pt(IV) complex $(PPN)_2[PtMe_3(P_3O_9)]$ (7) was also synthesised and structurally characterised.

Introduction

Considerable interest has been focussed on how the properties and reactivities of late transition metal complexes are modified on moving from the commonly used P- or N-donor ancillary ligand sets to the O-donor sets.[1–3] This originally stemmed from the intention of providing a correlation between atomic level structures and functions of the metal species on oxide surfaces in heterogeneous catalysts. More recently, silsesquioxane-[2] and polyoxometalate-supported[3] complexes of late transition metals have been found to show unique reactivities and catalytic activities; therefore O-donor ligands, particularly polyoxoanion ligands, have received increasing attention for their possibility of producing new types of catalytic materials. Among such poly-oxoanion ligands, we took note of cyclophosphates $(P_nO_{3n})^{n-}$. These anions comprise n corner-sharing PO_4 tetrahedra and have terminal P–O groups in a regular cyclic arrangement,[4] which is suitable for the model of the oxo surfaces in the heterogeneous oxide-supported catalysts. Inorganic salts of cyclophosphates have already been well-characterised for n = 3, 4, 5, 6, 8, 10 and 12, but their organometallic derivatives have not been investigated extensively. With respect to cyclotriphosphate ($P_3O_9{}^{3-}$), Klemperer has synthesised several organometallic complexes in his pioneering work.[5] For example, the anionic iridium complex with a $\kappa^3\text{-}P_3O_9$ ligand $[Ir(P_3O_9)(cod)]^{2-}$ (cod = 1,5-cyclooctadiene) has been reported to undergo unusual oxygenation with O_2 to form an oxametallabutane complex, where the flexidentate nature of the P_3O_9 ligand plays an important role in controlling the reaction course.[5e,6] However, examples of molecular complexes with this ligand have been limited to those of Group 4 (Hf[7b]), 7 (Mn,[5a,b] Re[5a,b]), 8 (Fe,[7a] Ru[5f,g,8]) and 9 (Rh,[5b] Ir[5c–e]) metals, and their synthetic methods with high generality still remain to be developed. In this article, we report the syntheses and structures of new P_3O_9 complexes of palladium and platinum, as well as their dynamic

behaviour in solution. In some complexes, relatively strong intramolecular CH $\cdots$ O hydrogen bonds are observed between the P_3O_9 and ancillary phosphine ligands.

Experimental

General methods

All manipulations were carried out under a dry nitrogen atmosphere by using standard Schlenk tube techniques. Solvents were dried by usual methods and distilled before use. $[PdCl_2(PPh_3)_2]$,[9] $[PdCl_2(PMePh_2)_2]$,[9] $[PtCl_2(PPh_3)_2]$,[10] $[PtCl_2(PMePh_2)_2]$,[10] $[PtCl_2(dppe)]$[11] [dppe = $Ph_2P(CH_2)_2PPh_2$], $[PtCl_2(dppb)]$[11] [dppb = $Ph_2P(CH_2)_4PPh_2$], $[PtMe_3I]_4$[12] and $(PPN)_3(P_3O_9)\cdot H_2O$[5d] [PPN = $(PPh_3)_2N^+$] were prepared according to the literature methods. Other reagents were commercially obtained and used without further purification. ^1H and $^{31}P-\{^1H\}$ NMR spectra were recorded on a JEOL JNM-EX-270 (^1H, 270 MHz; ^{31}P, 109 MHz), JEOL JNM-LA-400 (^1H, 400 MHz; ^{31}P, 162 MHz) or JEOL JNM-GSX-400 (^1H, 400 MHz) spectrometer, whilst IR spectra were recorded on a JASCO FT/IR-410 spectrometer. Elemental analyses were performed with a Perkin-Elmer 2400 series II CHN analyzer. The rates of intramolecular ligand exchange were estimated by using the computer program DNMR5,[13] and the calculated $^{31}P-\{^1H\}$ NMR spectra were visually compared to the experimental spectra.

Preparations

$(PPN)[Pd(P_3O_9)(PPh_3)_2]\cdot2.5CH_2Cl_2$ $(1\cdot2.5CH_2Cl_2)$. $AgPF_6$ (55.9 mg, 0.22 mmol) and $[PdCl_2(PPh_3)_2]$ (77.4 mg, 0.11 mmol) were dissolved in acetone (3.0 cm³) and stirred overnight at room temperature. After the precipitate was filtered off, the filtrate was evaporated to dryness *in vacuo*. To the residual solid were added $(PPN)_3(P_3O_9)\cdot H_2O$ (203 mg, 0.11 mmol) and

CH_2Cl_2 (4.0 cm³), and the mixture was stirred overnight at room temperature. The black precipitate that formed was filtered off, and the filtrate was evaporated under reduced pressure. The residue was extracted with MeOH and evaporated to dryness. The resultant solid was washed repeatedly with acetone and recrystallised from CH_2Cl_2–Et_2O to give yellow crystals of $1\cdot2.5CH_2Cl_2$. The X-ray diffraction study of this salt clearly showed that it contains 2.5 molecules of CH_2Cl_2 per complex anion. However, since the crystals are efflorescent, thoroughly dried samples were found to possess the empirical formula $1\cdot1.7CH_2Cl_2$. The yield after drying *in vacuo* was 21.2 mg (0.014 mmol, 13%). ν_{max}/cm⁻¹ (KBr): 1292s, 1267s, 1130m, 1117s, 1101m, 1070m, 998m, 981m, 957m. ³¹P–{¹H} NMR ($CDCl_3$, 20 °C): δ 33.2 (s, PPh_3), 21.1 (s, PPN), −15.9 (s, P_3O_9). ¹H NMR ($CDCl_3$, 20 °C): δ 7.17–7.73 (m, PPN and PPh_3). Found: C, 57.06; H, 4.32; N, 0.89; $C_{73.7}H_{63.4}Cl_{3.4}NO_9P_7Pd$ requires C, 57.08; H, 4.12; N, 0.90%.

(PPN)[Pd(P₃O₉)(PMePh₂)₂]·MeCN (2·MeCN). [PdCl₂(PMePh₂)₂] (172 mg, 0.30 mmol) was treated with $AgPF_6$ (151 mg, 0.60 mmol) in acetone (3.0 cm³) and then allowed to react with $(PPN)_3(P_3O_9)\cdot H_2O$ (552 mg, 0.30 mmol) in CH_2Cl_2 (3.0 cm³) as described above. The black precipitate was filtered off, and the filtrate was evaporated under reduced pressure. Recrystallisation of the resulting yellow solid from MeCN–Et_2O gave yellow crystals of 2·MeCN (263 mg, 0.20 mmol, 67%). ν_{max}/cm⁻¹ (KBr): 1295s, 1265s, 1135m, 1117s, 1104s, 1073m, 997s, 980s, 959m, 902m, 890m. ³¹P–{¹H} NMR ($CDCl_3$, 22 °C): δ 24.8 (s, PMePh₂), 21.1 (s, PPN), −15.8 (s, P_3O_9). ¹H NMR ($CDCl_3$, 22 °C): δ 7.19–7.67 (50 H, m, PPN and PMe*Ph₂*), 2.04 [6 H, d, ²*J*(PH) 12.0 Hz, P*Me*Ph₂]. Found: C, 57.81; H, 4.52; N, 1.91; $C_{64}H_{59}N_2O_9P_7Pd$ requires C, 58.08; H, 4.49; N, 2.12%.

(PPN)[Pt(P₃O₉)(PPh₃)₂]·2C₂H₄Cl₂ (3·2C₂H₄Cl₂). This compound was prepared from [PtCl₂(PPh₃)₂] and $(PPN)_3(P_3O_9)\cdot H_2O$ in a manner analogous to that described for $1\cdot2.5CH_2Cl_2$ except that 1,2-dichloroethane was used as the solvent for recrystallisation. Colorless crystals, 69% yield. ν_{max}/cm⁻¹ (KBr): 1297s, 1270s, 1130m, 1116s, 1102s, 1067m, 998s, 987s, 957m. ³¹P–{¹H} NMR ($CDCl_3$, 18 °C): δ 21.1 (s, PPN), 4.9 [s, ¹*J*(PtP) 4256 Hz, PPh₃], −16.8 (s, P_3O_9). ¹H NMR ($CDCl_3$, 18 °C): δ 7.17–7.73 (m, PPN and PPh_3). Found: C, 53.65; H, 4.23; N, 0.76; $C_{76}H_{68}Cl_4NO_9P_7Pt$ requires C, 53.92; H, 4.05; N, 0.83%. Crystals of $3\cdot2.5CH_2Cl_2$ suitable for X-ray analysis were obtained by further recrystallisation from CH_2Cl_2–Et_2O.

(PPN)[Pt(P₃O₉)(PMePh₂)₂]·MeCN (4·MeCN). This compound was prepared from [PtCl₂(PMePh₂)₂] and $(PPN)_3(P_3O_9)\cdot H_2O$ in a manner similar to that described for 2·MeCN. Colorless crystals, 57% yield. ν_{max}/cm⁻¹ (KBr): 1296s, 1271s, 1255s, 1134m, 1116s, 1105s, 1070m, 984s, 961m, 903m, 894m. ³¹P–{¹H} NMR ($CDCl_3$, 18 °C): δ 21.0 (s, PPN), −5.4 [s, ¹*J*(PtP) 4156 Hz, PMePh₂], −16.4 (s, P_3O_9). ¹H NMR ($CDCl_3$, 18 °C): δ 7.19–7.68 (50 H, m, PPN and PMe*Ph₂*), 1.96 [6H, d, ²*J*(PH) 11.7 Hz, P*Me*Ph₂]. Found: C, 54.39; H, 4.39; N, 1.79; $C_{64}H_{59}N_2O_9P_7Pt$ requires C, 54.44; H, 4.21; N, 1.98%.

(PPN)[Pt(P₃O₉)(dppe)]·0.5MeCN·0.5CH₂Cl₂ (5·0.5MeCN·0.5CH₂Cl₂). This compound was prepared from [PtCl₂(dppe)] and $(PPN)_3(P_3O_9)\cdot H_2O$ in a manner similar to that described for 2·MeCN except that pure samples were obtained by addition of Et_2O to a MeCN/CH_2Cl_2 (3/2 v/v) solution. Colorless crystals, 52% yield. ν_{max}/cm⁻¹ (KBr): 1310s, 1293s, 1266s, 1132m, 1116s, 1105m, 1069m, 997m, 987m, 962m. ³¹P–{¹H} NMR (CD_2Cl_2, 18 °C): δ 31.3 [s, ¹*J*(PtP) 4063 Hz, dppe], 20.8 (s, PPN), −16.4 (s, P_3O_9). ¹H NMR (CD_2Cl_2, 24 °C): δ 7.46–8.06 (50 H, m, Ph of PPN and dppe), 2.33 [4 H, br d, ²*J*(PH) 17.6 Hz, CH₂ of dppe]. Found: C, 53.58; H, 4.10; N, 1.24; $C_{63.5}H_{56.5}ClN_{1.5}O_9P_7Pt$ requires C, 53.26; H, 3.98; N, 1.47%. The corresponding tetraphenylphosphonium salt

(PPh₄)[Pt(P₃O₉)(dppe)]·MeCN·0.5CH₂Cl₂ (5′·MeCN·0.5CH₂-Cl₂), which was used for X-ray analysis, was obtained by anion metathesis of 5 with PPh₄Cl and recrystallisation by slow diffusion of hexane into a MeCN/CH_2Cl_2 (1/3 v/v) solution of the PPh₄ salt.

(PPN)[Pt(P₃O₉)(dppb)]·MeCN·0.5CH₂Cl₂ (6·MeCN·0.5CH₂Cl₂). This compound was prepared from [PtCl₂(dppb)] and $(PPN)_3(P_3O_9)\cdot H_2O$ in a manner similar to that described for 2·MeCN except that pure samples were obtained by addition of Et_2O to a MeCN/CH_2Cl_2 (2/1 v/v) solution. Colorless crystals, 42% yield. ν_{max}/cm⁻¹ (KBr): 1296s, 1269s, 1129m, 1117s, 1104m, 1069m, 997m, 983s, 957m. ³¹P–{¹H} NMR (CD_2Cl_2, 20 °C): δ 20.8 (s, PPN), 1.95 [s, ¹*J*(PtP) 3995 Hz, dppb], −17.3 (s, P_3O_9). ¹H NMR (CD_2Cl_2, 21 °C): δ 7.33–7.74 (50 H, m, Ph of PPN and dppb), 2.46, 2.07 (4 H each, br, CH₂ of dppb). Found: C, 54.27; H, 4.35; N, 1.98; $C_{66.5}H_{62}ClN_2O_9P_7Pt$ requires C, 53.95; H, 4.22; N, 1.89%.

(PPN)₂[PtMe₃(P₃O₉)] (7). A mixture of [PtMe₃I]₄ (51.5 mg, 0.035 mmol) and $(PPN)_3(P_3O_9)\cdot H_2O$ (261 mg, 0.14 mmol) in CH_2Cl_2 (3.0 cm³) was stirred overnight at room temperature. Then the reaction mixture was filtered, and the filtrate was evaporated to dryness *in vacuo*. The residual solid was washed with acetone and recrystallised from CH_2Cl_2–Et_2O to give colorless crystals of 7 (151 mg, 0.097 mmol, 70%). ν_{max}/cm⁻¹ (KBr): 1327m, 1297s, 1272s, 1116s, 996m, 983m, 954m. ³¹P–{¹H} NMR ($CDCl_3$, 17 °C): δ 21.1 (s, PPN), −9.3 [s, ²*J*(PtP) 63 Hz, P_3O_9]. ¹H NMR ($CDCl_3$, 17 °C): δ 7.44–7.69 (60 H, m, PPN), 1.02 [9 H, s, ²*J*(PtH) 79 Hz, Me]. Found: C, 58.29; H, 4.52; N, 1.86; $C_{75}H_{69}N_2O_9P_7Pt$ requires C, 57.96; H, 4.47; N, 1.80%.

Crystallography

For $3\cdot2.5CH_2Cl_2$, diffraction data were collected at −170 °C on a Rigaku RAXIS RAPID imaging plate area detector with graphite monochromatised Mo-Kα radiation (λ = 0.71069 Å) to a maximum 2θ value of 54.9°. For the other compounds, data were collected at room temperature on a Rigaku AFC7R four-circle automated diffractometer with graphite monochromatised Mo-Kα radiation using the ω–2θ scan technique to a maximum 2θ value of 50° (for $1\cdot2.5CH_2Cl_2$) or 55° (except for $1\cdot2.5CH_2Cl_2$). Details of the crystals and data collection parameters are summarised in Table 1.

The structure solution and refinements were carried out by using teXsan [14] and CrystalStructure [15] crystallographic software packages. The positions of non-hydrogen atoms were determined by Patterson methods (DIRDIF PATTY [16]) or direct methods (SIR92 [17]) and expanded using Fourier techniques (DIRDIF-94 [18] or -99 [19]). For $1\cdot2.5CH_2Cl_2$ and $3\cdot2.5CH_2Cl_2$, the carbon atoms of the solvating CH_2Cl_2 molecules were refined isotropically. In each case one of the CH_2Cl_2 molecules was found to be located on the centre of symmetry; the carbon atom for this CH_2Cl_2 molecule was refined with a 50% occupancy. For $5′\cdot MeCN\cdot0.5CH_2Cl_2$ and $6\cdot MeCN\cdot0.5CH_2Cl_2$, the CH_2Cl_2 molecules were found to be located near the centre of symmetry. For the CH_2Cl_2 molecule in $5′\cdot MeCN\cdot0.5CH_2Cl_2$, the chlorine atoms were refined anisotropically with a 50% occupancy, whilst the carbon atoms were included in the refinement with fixed isotropic parameters with a 50% occupancy. The disordered carbon and chlorine atoms of the CH_2Cl_2 molecule in $6\cdot MeCN\cdot0.5CH_2Cl_2$ were treated with fixed isotropic parameters with a 50% occupancy. All the other non-hydrogen atoms were refined by full-matrix least-squares techniques with anisotropic thermal parameters. Hydrogen atoms except for those of the disordered CH_2Cl_2 molecules in $3\cdot2.5CH_2Cl_2$ and $6\cdot MeCN\cdot0.5CH_2Cl_2$ were placed at calculated positions (d_{C-H} = 0.95 Å) and included in the final stages of refinements with fixed parameters.

Table 1 Crystal data for complexes **1–7**

	1·2.5CH₂Cl₂	2·MeCN	3·2.5CH₂Cl₂	4·MeCN	5'·MeCN·0.5CH₂Cl₂	6·MeCN·0.5CH₂Cl₂	7
Formula	$C_{74.5}H_{65}PdP_7O_9NCl_5$	$C_{64}H_{59}PdP_7O_9N_2$	$C_{74.5}H_{65}PtP_7O_9NCl_5$	$C_{64}H_{59}PtP_7O_9N_2$	$C_{52.5}H_{48}PtP_7O_9NCl$	$C_{66.5}H_{62}PtP_7O_9N_2Cl$	$C_{75}H_{69}N_2O_9P_7Pt$
M	1618.82	1323.39	1707.51	1412.08	1253.34	1480.59	1492.34
Crystal system	Triclinic	Triclinic	Triclinic	Triclinic	Triclinic	Monoclinic	Monoclinic
Space group	$P\bar{1}$ (no. 2)	$P\bar{1}$ (no. 2)	$P\bar{1}$ (no. 2)	$P\bar{1}$ (no. 2)	$P\bar{1}$ (no. 2)	$P2_1/c$ (no. 14)	Cc (no. 9)
a/Å	14.19(1)	12.690(6)	14.1829(7)	12.687(1)	9.939(1)	19.420(4)	29.960(8)
b/Å	16.079(6)	14.844(4)	15.9737(4)	14.866(2)	15.728(2)	17.066(3)	13.177(9)
c/Å	17.426(5)	18.925(5)	17.0641(7)	18.923(2)	17.660(2)	20.321(3)	21.038(7)
α/°	105.52(3)	106.07(2)	105.188(2)	106.24(1)	103.29(1)		
β/°	92.75(4)	97.30(4)	92.784(2)	97.076(9)	95.04(1)	104.99(1)	122.45(2)
γ/°	103.84(5)	109.98(3)	103.9060(9)	110.016(9)	93.56(1)		
V/Å³	3693(3)	3121(2)	3595.8(3)	3123.3(9)	2666.5(7)	6505(2)	7008(5)
Z	2	2	2	2	2	4	4
μ(MoKα)/cm⁻¹	6.40	5.34	23.43	24.74	29.06	24.19	21.66
D_c/g cm⁻³	1.455	1.408	1.577	1.501	1.561	1.512	1.414
No. unique data	13005	14327	15499	14339	12226	14959	8050
R_{int}	0.043	0.016	0.032	0.026	0.018	0.026	0.058
No. data used [$I > \sigma(I)$]	7283	9596	13232	10966	9598	9237	
No. variables	869	748	932	749	638	767	849
R; $R_w{}^a$	0.050; 0.051	0.035; 0.035	0.028; 0.039	0.031; 0.032	0.031; 0.032	0.038; 0.039	0.073; 0.092^b

^{a} $R = \Sigma||F_o| - |F_c||/\Sigma|F_o|$; $R_w = [\Sigma w(|F_o| - |F_c|)^2/\Sigma w F_o^2]^{1/2}$. For all data, $R = \Sigma(F_o^2 - F_c^2)/\Sigma F_o^2$, $R_w = [\Sigma w(F_o^2 - F_c^2)^2/\Sigma w(F_o^2)^2]^{1/2}$. ^{b}

CCDC reference numbers 202873–202879.

See http://www.rsc.org/suppdata/dt/b3/b301223a/ for crystallographic data in CIF or other electronic format.

Results and discussion

Syntheses and structures of (PPN)[Pd(P₃O₉)(PPh₃)₂] (1) and (PPN)[Pd(P₃O₉)(PMePh₂)₂] (2)

Our initial attempts to synthesise Pd(II) P₃O₉ complexes with diene ligands resulted in the formation of products unstable at room temperature, although the Rh(I) and Ir(I) analogues have been known for some time.[5b–e] In contrast, use of phosphines as the ancillary ligands produced much more stable P₃O₉ complexes of palladium. Thus, the P₃O₉³⁻ as a PPN salt smoothly reacted with the cationic solvated palladium complex [Pd(Me₂CO)₂(PPh₃)₂](PF₆)₂[20] in CH₂Cl₂ at room temperature to form the anionic complex (PPN)[Pd(P₃O₉)(PPh₃)₂] (**1**), which was isolated as air-stable yellow crystals (Scheme 1). The structure of **1**·2.5CH₂Cl₂ was established by X-ray crystallography [Fig. 1(a)]. Selected bond lengths and angles are given in Table 2.


Scheme 1
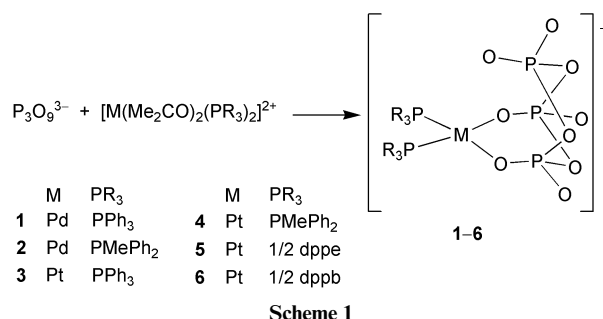
The palladium atom is coordinated by the two phosphine ligands and two oxygen atoms of the P₃O₉ ligand with a square-planar geometry [Pd–O(1) = 2.089(4), Pd–O(2) = 2.078(4), Pd–P(4) = 2.258(2), Pd–P(5) = 2.267(2) Å] and has an additional weak interaction with another oxygen atom [O(3)] of the P₃O₉ ligand [Pd ⋯ O(3) = 2.902(5) Å]. This Pd ⋯ O(3) distance is considerably longer than the corresponding Rh–O [2.343(5) Å] and Ir–O [2.70(2) Å] distances in [NBuⁿ₄]₂[Rh(P₃O₉)(nbd)] (nbd = 2,5-norbornadiene)[5b] and [NBuⁿ₄]₂[Ir(P₃O₉)(cod)],[5c] but is comparable to those of Pd ⋯ O weak interactions found in Pd(II) complexes such as [Pd(C₆H₄CH₂NMe₂-C²,N)Cl-{P[C₆H₃(OMe)₂]₃}] [Pd ⋯ O = 2.920(8) Å].[21] With this interaction, the coordination structure around the palladium centre may be regarded as a highly distorted square pyramid. Due to this coordination mode of the tripodal P₃O₉ ligand, the P(3)–O(3) bond [1.480(4) Å] is shorter than the other coordinating P–O units [P(1)–O(1) = 1.509(4), P(2)–O(2) = 1.502(4) Å] but is slightly longer than the non-coordinating equatorial P–O$_{terminal}$ bonds [1.455(4)–1.460(5) Å].

The O(3) atom is also located very close to two *ortho* CH groups of the PPh₃ ligands [O(3) ⋯ C(2) = 3.185(9), O(3) ⋯ H(1) = 2.25 Å, O(3) ⋯ H(1)–C(2) = 167.3°; O(3) ⋯ C(20) = 3.216(9), O(3) ⋯ H(16) = 2.34 Å, O(3) ⋯ H(16)–C(20) = 154.0°; the C–H bond distances are normalised to 0.95 Å], and these contacts are regarded as intramolecular CH ⋯ O hydrogen bonds.[22] With this type of interaction, the C ⋯ O (*D*) and H ⋯ O (*d*) contacts usually fall in the range of 3.0 < *D* < 4.0 Å and 2.0 < *d* < 3.0 Å, respectively. In **1**, the estimated O ⋯ H distances are significantly short (2.3 Å) and the O ⋯ H–C angles are close to linearity (>150°). These metrical features indicate that the O(3) atom forms relatively strong intramolecular CH ⋯ O hydrogen bonds. Some of the oxygen atoms in the P₃O₉ ligand also have short non-bonding contacts with CH groups in the PPN cation and solvating CH₂Cl₂ molecules. For example, the O(2) and O(3) atoms lie close to the C(39)–H(32) and C(71)–

**Table 2** Selected bond distances (Å) and angles (°) in complexes **1–6**

	1·2.5CH₂Cl₂ᵃ	2·MeCNᵃ	3·2.5CH₂Cl₂ᵇ	4·MeCNᵇ	5'·MeCN·0.5CH₂Cl₂ᵇ	6·MeCN·0.5CH₂Cl₂ᵇ
M–O(1)	2.089(4)	2.081(2)	2.076(2)	2.082(2)	2.093(3)	2.084(3)
M–O(2)	2.078(4)	2.107(2)	2.091(2)	2.100(2)	2.090(3)	2.101(4)
M–O(3)	2.902(5)	2.838(2)	3.030(2)	3.032(4)	4.131(6)	3.030(4)
M–P(4)	2.258(2)	2.229(1)	2.236(1)	2.217(1)	2.217(1)	2.216(1)
M–P(5)	2.267(2)	2.2397(8)	2.232(1)	2.221(1)	2.208(1)	2.222(1)
P(1)–O(1)	1.509(4)	1.509(2)	1.513(2)	1.511(3)	1.506(3)	1.512(4)
P(1)–O(4)	1.455(4)	1.459(2)	1.468(2)	1.457(3)	1.456(3)	1.465(4)
P(2)–O(2)	1.502(4)	1.508(2)	1.522(2)	1.506(3)	1.508(3)	1.515(4)
P(2)–O(6)	1.458(4)	1.456(2)	1.462(2)	1.457(3)	1.453(3)	1.457(4)
P(3)–O(3)	1.480(4)	1.473(2)	1.476(2)	1.472(3)	1.413(4)	1.471(4)
P(3)–O(8)	1.460(5)	1.461(2)	1.467(2)	1.463(3)	1.439(4)	1.465(4)
P(4)–M–P(5)	97.84(7)	98.38(3)	98.38(3)	99.69(4)	86.52(4)	93.74(5)
P(4)–M–O(1)	176.3(1)	174.77(6)	171.34(6)	173.12(8)	177.78(8)	171.0(1)
P(4)–M–O(2)	88.5(1)	83.37(6)	84.59(6)	83.50(7)	92.27(8)	87.2(1)
P(5)–M–O(1)	84.1(1)	86.25(6)	88.65(7)	86.24(7)	91.66(7)	90.1(1)
P(5)–M–O(2)	170.4(1)	166.56(6)	176.43(6)	169.74(7)	178.68(9)	177.7(1)
O(1)–M–O(2)	89.1(2)	92.69(7)	88.22(9)	91.26(10)	89.57(10)	88.7(1)

ᵃ M = Pd. ᵇ M = Pt.
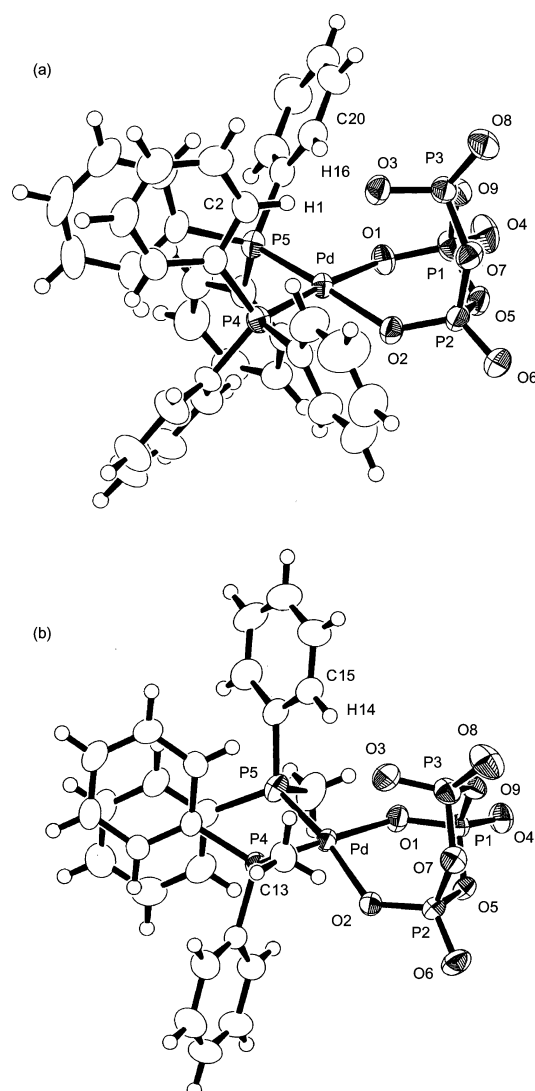
Fig. 1 The molecular structures of the anionic parts of **1**·2.5CH₂Cl₂ (a) and **2**·MeCN (b). Solvating molecules are omitted for clarity.

H(59) groups of the PPN cation, respectively [O(2) ··· C(39) = 3.376(8), O(2) ··· H(32) = 2.44 Å, O(2) ··· H(32)–C(39) = 169.1°; O(3) ··· C(71) = 3.273(9), O(3) ··· H(59) = 2.41 Å, O(3) ··· H(59)–C(71) = 151.4°], whilst the O(6) atom approaches the C(73)–H(62) of one of the solvated CH₂Cl₂ molecules [O(6) ··· C(73) = 3.20(1), O(6) ··· H(62) = 2.26 Å,

O(6) ··· H(62)–C(73) = 171.7°]. We consider that the strong tendency of the P₃O₉ ligand to form CH ··· O hydrogen bonds has a crucial effect on controlling the conformation of its complexes at least in the solid state.

The ³¹P–{¹H} NMR spectrum of **1** at ambient temperature displays only one phosphorus resonance for the P₃O₉ ligand at δ −15.9 in spite of its local C_s structure in the solid state. The equivalence of the phosphorus atoms is accounted for by a rapid intramolecular ligand exchange process involving the hapticity change and pseudo-rotation of the P₃O₉ ligand (Scheme 2). However, the ³¹P–{¹H} NMR spectrum shows essentially no line broadening on cooling to −60 °C. This fluxional behaviour is similar to that observed for the above-mentioned anionic iridium complex [Ir(P₃O₉)(cod)]²⁻.[5c]
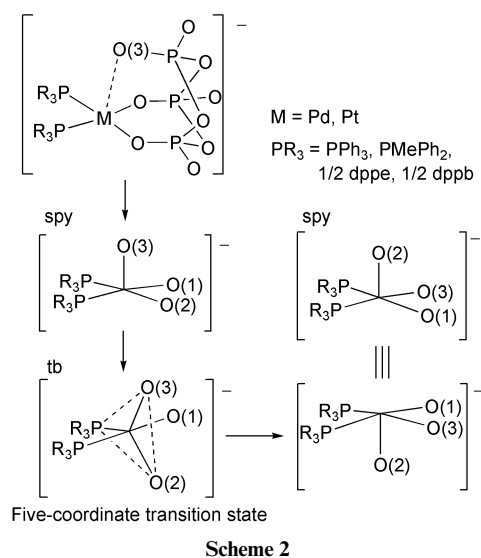
Scheme 2

It is expected that use of more electron-donating ancillary ligands disfavors the coordination of the third oxygen atom and decelerates the ligand exchange process. Since the dynamic behaviour of metal complexes involving the hapticity change of flexidentate ligands has been attracting intense research activity,[22–24] we have synthesised the PMePh₂ analogue of **1**. The reaction of the cationic solvated complex [Pd(Me₂CO)₂(PMePh₂)₂](PF₆)₂ with (PPN)₃(P₃O₉) in CH₂Cl₂ at room temperature gave (PPN)[Pd(P₃O₉)(PMePh₂)₂] (**2**) in good yield. The structure of **2**·MeCN has been confirmed by X-ray crystallography [Fig. 1(b)]. Selected bond distances and angles are given in Table 2.

The coordination structure around the palladium atom in **2** is similar to that of **1** [Pd–O(1) = 2.081(2), Pd–O(2) = 2.107(2), Pd–P(4) = 2.229(1), Pd–P(5) = 2.2397(8) Å], and the palladium centre has a weak interaction with the third oxygen atom [O(3)] of the P_3O_9 ligand [Pd ⋯ O(3) = 2.838(2) Å]. Again, the O(3) atom forms intramolecular CH ⋯ O hydrogen bonds with one methyl and one phenyl group of the $PMePh_2$ ligands [O(3) ⋯ C(13) = 3.239(4), O(3) ⋯ C(15) = 3.425(4) Å], although the O ⋯ C non-bonding separations are somewhat longer than those found in **1**. The $^{31}P-\{^{1}H\}$ NMR spectrum of **2** at ambient temperature also exhibits only one phosphorus resonance attributable to the P_3O_9 ligand at δ −15.8, and unfortunately no temperature dependence is observed.

Syntheses and structures of (PPN)[Pt(P₃O₉)(PPh₃)₂] (3) and (PPN)[Pt(P₃O₉)(PMePh₂)₂] (4)

It is known that the rate of ligand substitution is often faster for Pd(II) than for Pt(II).[24] So we changed the central metal from palladium to platinum in order to gain further insights into the intramolecular ligand exchange process in the P_3O_9 complexes. The platinum complexes (PPN)[Pt(P₃O₉)(PPh₃)₂] (**3**) and (PPN)[Pt(P₃O₉)(PMePh₂)₂] (**4**) were synthesised by the reaction of (PPN)₃(P₃O₉) with the cationic solvated complexes [Pt(Me₂CO)₂(PPh₃)₂](PF₆)₂ and [Pt(Me₂CO)₂(PMePh₂)₂](PF₆)₂, respectively, and were isolated as stable colorless crystals (Scheme 1). The structures of **3** and **4** have been established by X-ray diffraction study as depicted in Fig. 2, and selected bond distances and angles are summarised in Table 2.

The crystals of **3**·2.5CH₂Cl₂ and **4**·MeCN are isomorphic with those of the palladium complexes **1**·2.5CH₂Cl₂ and **2**·MeCN, respectively. In both **3** and **4**, the platinum centre is coordinated by P_2O_2 donor atoms with a square-planar geometry and has an additional weak interaction with the third oxygen atom [O(3)] in the P_3O_9 ligand, where the Pt ⋯ O(3) separation [3.030(2) Å for **3**, 3.032(4) Å for **4**] is slightly longer than the corresponding Pd ⋯ O distance in **1** and **2**. The O(3) atom is also engaged in intramolecular CH ⋯ O hydrogen bonds with phosphine CH groups. In particular, the O(3) ⋯ H(1)–C(2) and O(3) ⋯ H(16)–C(20) interactions in **3** may be regarded as relatively strong CH ⋯ O hydrogen bonds [O(3) ⋯ C(2) = 3.201(4), O(3) ⋯ H(1) = 2.32 Å, O(3) ⋯ H(1)–C(2) = 154.8°; O(3) ⋯ C(20) = 3.211(4), O(3) ⋯ H(16) = 2.28 Å, O(3) ⋯ H(16)–C(20) = 167.2°].

The $^{31}P-\{^{1}H\}$ NMR spectra of **3** and **4** at room temperature are similar to those of **1** and **2**, showing one signal attributable to the P_3O_9 ligand at δ −16.8 and −16.4, respectively. The signal of **3** is broadened at −60 °C in CDCl₃, although we could not observe complete coalescence. In contrast, the P_3O_9 signal of **4** in CD₂Cl₂ coalesces at −70 °C and splits into two broad signals at −90 °C [δ −14.1 (2 P), −24.1 (1 P)]. These observations clearly indicate that the intramolecular ligand exchange process is slower for the platinum complexes **3** and **4** than for their palladium analogues.

Syntheses and structures of (PPN)[Pt(P₃O₉)(dppe)] (5) and (PPN)[Pt(P₃O₉)(dppb)] (6)

We have further turned our attention to P_3O_9 complexes of platinum with a chelate phosphine ligand, because the chelate ring size and the bridge structure of the ancillary diphosphine ligand have been documented to possess profound effects on the dynamic behaviour of Tp^{iPr2} (Tp^{iPr2} = hydrotris-3,5-diisopropylpyrazolylborato) complexes of rhodium [Tp^{iPr2}Rh-(diphosphine)] (*vide infra*).[25] (PPN)[Pt(P₃O₉)(dppe)] (**5**) and (PPN)[Pt(P₃O₉)(dppb)] (**6**) were synthesised from the cationic solvated complexes [Pt(Me₂CO)₂(dppe)](OTf)₂ and [Pt(Me₂-CO)₂(dppb)](OTf)₂, respectively, by the reaction with (PPN)₃(P₃O₉) in CH₂Cl₂ at room temperature (Scheme 1). The structure of [Pt(P₃O₉)(dppe)]⁻ ion has been determined by the X-ray crystallographic study of the tetraphenylphosphonium
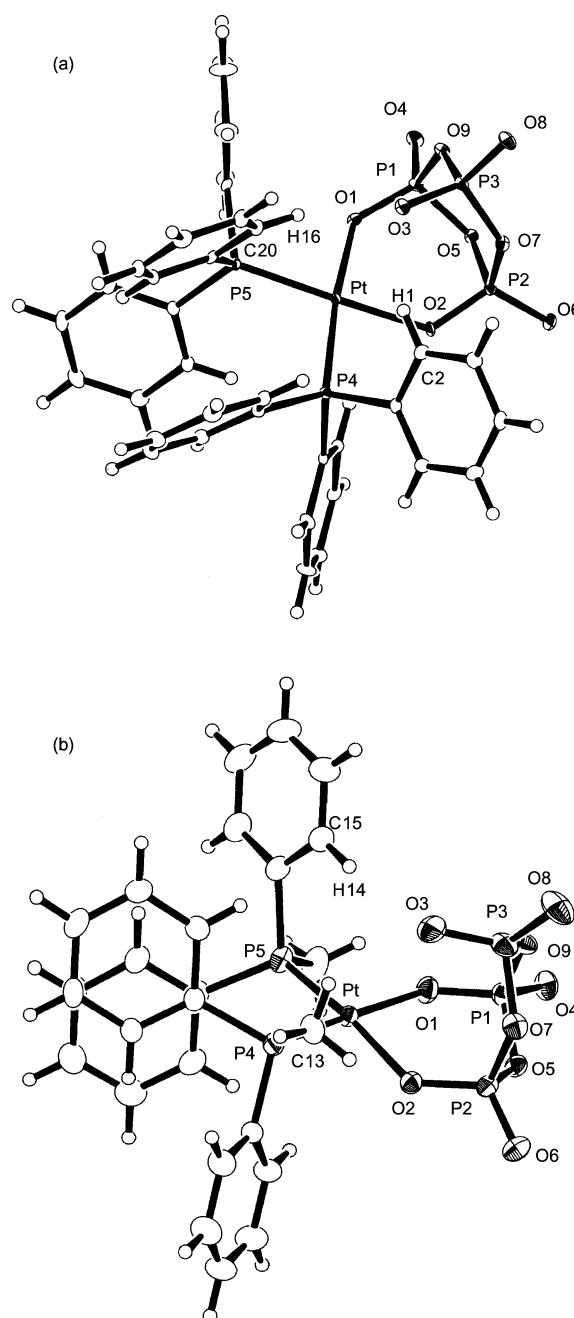

Fig. 2 The molecular structures of the anionic parts of **3**·2.5CH₂Cl₂ (a) and **4**·MeCN (b). Solvating molecules are omitted for clarity.

salt **5′**·MeCN·0.5CH₂Cl₂ derived from **5**, whilst recrystallisation of **6** directly gave crystals suitable for diffraction study. Selected bond lengths and angles are given in Table 2, and ORTEP[26] drawings for the anions are in Fig. 3.

In **5′**, the conformation of the P_3O_9 ligand is deformed from a chair form to a pseudo-boat, where the P(1)–O(9)–P(3)–O(7)–P(2) part of the six-membered ring is almost planar. This type of structure has not been found previously in crystallographically characterised P_3O_9 complexes, but we assume that the pseudo-boat conformation of the P_3O_9 ligand reflects the conformational flexibility of the P_3O_3 ring. This deformation is considered to be the result of steric congestion between the dppe and P_3O_9 ligands. Consequently, the O(3) atom moves away from the platinum centre; the large Pt ⋯ O(3) separation [4.131(6) Å] precludes any bonding interaction between these atoms. Thus the platinum centre takes a normal square-planar coordination structure. It would also be interesting to point out that the P(3)–O(3) distance in **5′** [1.413(4) Å] is noticeably shorter than those in complexes **1**–**4**.
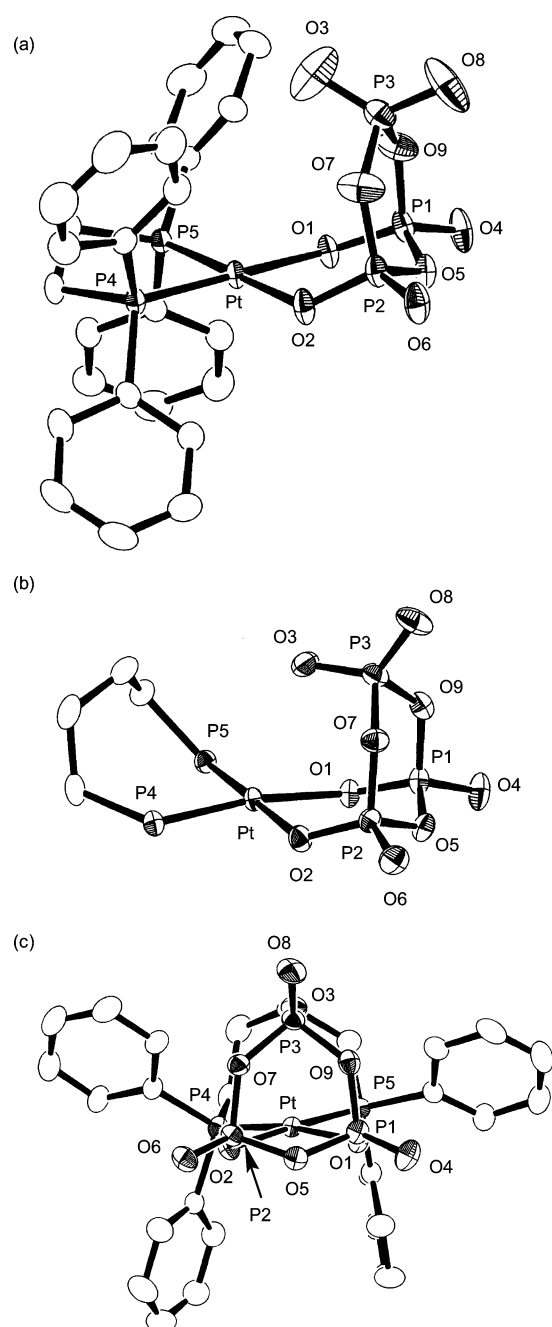
Fig. 3 The molecular structures of the anionic parts of **5′·MeCN·0.5CH₂Cl₂** (a) and **6·MeCN·0.5CH₂Cl₂** (b) and (c) (side view to show the arrangement of phenyl groups). Solvating molecules, all hydrogen atoms and phenyl carbon atoms in (b) are omitted for clarity.

Scheme 3

In the ^{31}P–{^{1}H} NMR spectrum of **5** in CD₂Cl₂, one singlet resonance (δ −16.4) is observed for the P₃O₉ ligand at room temperature, but this signal coalesces at −50 °C and is further changed into two broad signals [δ −13.0 (2 P), −24.3 (1 P)] at −90 °C. The higher coalescence temperature of **5** than those of **3** and **4** is accounted for by the pseudo-boat conformation of the P₃O₉ ligand in **5**, where the large Pt · · · O(3) separation substantiates the difficulty in forming the penta-coordinate Pt centre (Scheme 3). Such steric deceleration is considered to be typical of a dynamic process by an associative mechanism.[25]

In contrast to **5′**, **6** takes a coordination structure similar to those of **1–4**. Thus, the platinum atom resides at the centre of the P₂O₂ donor atoms with a square-planar geometry and in addition is weakly coordinated by the third oxygen atom [O(3)] of the P₃O₉ ligand. The Pt · · · O(3) distance of 3.030(4) Å is comparable to those in **3** and **4**. The (CH₂)₄ bridge of the dppb ligand is folded upward from the PtO₂P₂ coordination plane, and in compensation for this, the two Ph groups take a widely
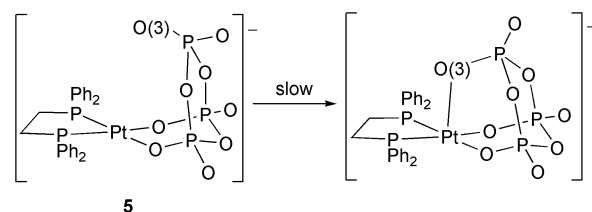
opened arrangement. Obviously this conformation enables the O(3) atom of the P₃O₉ ligand to approach the platinum centre. A similar folded chelate structure of dppb has also been found in [PdCl₂(dppb)].[27]

In the ^{31}P–{^{1}H} NMR spectrum of **6** in CD₂Cl₂ at room temperature, the signal of the P₃O₉ ligand appears again as one singlet at δ −17.3, but this signal coalesces at −40 °C and is split into a set of one doublet [δ −14.6, 2 P, ^2J(PP) 26 Hz] and one triplet [δ −23.6, 1 P, ^2J(PP) 26 Hz] at −95 °C, which is in full agreement with the solid state structure.

Akita and co-workers have revealed that the (CH₂)$_n$ bridge in the diphosphine ligands in related square-planar hydrotris-(pyrazolyl)borato complexes [Tp^{iPr2}Rh(diphosphine)] is folded toward the apical position.[25] They have concluded that the steric repulsion between the folded (CH₂)$_n$ bridge and the pendant pyrazole ring disfavors the penta-coordinate structure of the rhodium centre and consequently retards intramolecular ligand exchange processes. In contrast, the sterically less demanding P₃O₉ ligand can interact with the platinum centre irrespective of the steric effect of the (CH₂)₄ bridge in the dppb ligand in **6** [Fig. 3(b)]. Nevertheless, judging from the temperature dependence of the ^{31}P–{^{1}H} NMR spectra, the intramolecular ligand exchange process of **6** is much slower than that of **3** and **4**. We have concluded that this is a consequence of the slow pseudo-rotation process of the penta-coordinate intermediate. As shown in Scheme 4, simple pseudo-rotation of
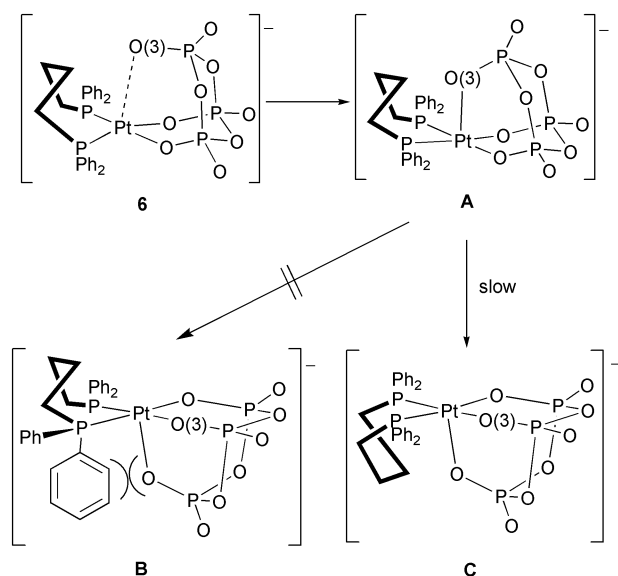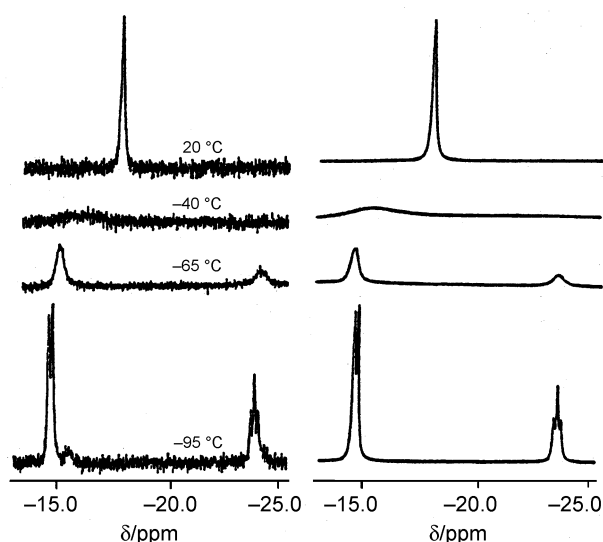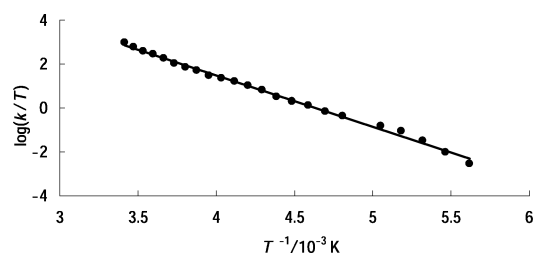

Scheme 4

the square-pyramidal intermediate leads to the sterically unsuitable relative arrangement of the folded (CH₂)₄ bridge and the apical coordination site (B). To complete the exchange process, it is necessary to invert the dppb chelate ring during the pseudo-rotation (A → C), which we assume to be unfavorable for the sterically congested penta-coordinate state of **6**.

The exchange rates for **6** at different temperatures were determined by comparing the computer-simulated ^{31}P–{^{1}H} NMR spectra with the experimental data (Fig. 4). An Eyring plot of the temperature dependence of the rate constants

Table 3 Selected bond distances (Å) and angles (°) in complex **7**

Pt–O(1)	2.191(8)	Pt–O(2)	2.197(6)
Pt–O(3)	2.223(7)	Pt–C(1)	2.05(1)
Pt–C(2)	2.002(10)	Pt–C(3)	2.00(1)
P(1)–O(1)	1.492(9)	P(2)–O(2)	1.510(6)
P(3)–O(3)	1.478(7)		
O(1)–Pt–O(2)	89.0(2)	O(1)–Pt–O(3)	88.8(3)
O(2)–Pt–O(3)	88.3(2)		

Fig. 6 The molecular structure of the anionic part of **7**. All hydrogen atoms are omitted for clarity.

cation [O(8) ⋯ C(66) = 3.14(1), O(8) ⋯ H(61) = 2.27 Å, O(8) ⋯ H(61)–C(66) = 150.4°], and this contact may be regarded as a relatively strong CH ⋯ O hydrogen bond.

References

1 P. R. Sharp, *J. Chem. Soc., Dalton Trans.*, 2000, 2647.
2 F. J. Feher and T. A. Budzichowski, *Polyhedron*, 1995, **14**, 3239; R. Murugavel, A. Voigt, M. G. Walawalkar and H. W. Roesky, *Chem. Rev.*, 1996, **96**, 2205; E. A. Quadrelli, J. E. Davies, B. F. G. Johnson and N. Feeder, *Chem. Commun.*, 2000, 1031; B. Marciniec and H. Maciejewski, *Coord. Chem. Rev.*, 2001, **223**, 301.
3 H. Weiner and R. G. Finke, *J. Am. Chem. Soc.*, 1999, **121**, 9831; H. Weiner, Y. Hayashi and R. G. Finke, *Inorg. Chem.*, 1999, **38**, 2579.
4 A. Durif, *Crystal Chemistry of Condensed Phosphates*, Plenum Press, New York, 1995.
5 (*a*) C. J. Besecker and W. G. Klemperer, *J. Organomet. Chem.*, 1981, **205**, C31; (*b*) C. J. Besecker, V. W. Day and W. G. Klemperer, *Organometallics*, 1985, **4**, 564; (*c*) V. W. Day, W. G. Klemperer and D. J. Main, *Inorg. Chem.*, 1990, **29**, 2345; (*d*) W. G. Klemperer and D. J. Main, *Inorg. Chem.*, 1990, **29**, 2355; (*e*) V. W. Day, W. G. Klemperer, S. P. Lockledge and D. J. Main, *J. Am. Chem. Soc.*, 1990, **112**, 2031; (*f*) V. W. Day, T. A. Eberspacher, W. G. Klemperer, R. P. Planalp, P. W. Schiller, A. Yagasaki and B. Zhong, *Inorg. Chem.*, 1993, **32**, 1629; (*g*) W. G. Klemperer and B. Zhong, *Inorg. Chem.*, 1993, **32**, 5821.
6 V. W. Day, T. A. Eberspacher, W. G. Klemperer and B. Zhong, *J. Am. Chem. Soc.*, 1994, **116**, 3119.
7 (*a*) K.-N. Han, D. Whang, H.-J. Lee, Y. Do and K. Kim, *Inorg. Chem.*, 1993, **32**, 2597; (*b*) S. Ryu, D. Whang, J. Kim, W. Yeo and K. Kim, *J. Chem. Soc., Dalton Trans.*, 1993, 205.
8 D. Attanasio, F. Bachechi and L. Suber, *J. Chem. Soc., Dalton Trans.*, 1993, 2373.
9 J. M. Jenkins and B. L. Shaw, *J. Chem. Soc. A*, 1966, 770.
10 J. A. Rahn, L. Baltusis and J. H. Nelson, *Inorg. Chem.*, 1990, **29**, 750.
11 M. Hacket and G. Whitesides, *J. Am. Chem. Soc.*, 1988, **110**, 1449.
12 J. C. Baldwin and W. C. Kaska, *Inorg. Chem.*, 1975, **14**, 2020.
13 D. S. Stephenson and G. Binsch, Program QCPE365; Quantum Chemistry Program Exchange, Indiana University, Bloomington, 1978.
14 teXsan, Crystal Structure Analysis Package, Molecular Structure Corporation, Houston, TX, 1985 & 1999.
15 CrystalStructure 3.00, Crystal Structure Analysis Package, Rigaku and Rigaku/MSC, Tokyo, Japan, 2000–2002.
16 P. T. Beurskens, G. Admiraal, G. Beurskens, W. P. Bosman, S. Garsia-Granda, R. O. Gould, J. M. M. Smits and C. Smykalla, The DIRDIF program system, Technical Report of the Crystallography Laboratory, University of Nijmegen, The Netherlands, 1992.
17 A. Altomare, G. Cascarano, C. Giacovazzo, A Guagliardi, M. Burla, G. Polidori and M. Camalli, *J. Appl. Crystallogr.*, 1994, **27**, 435.
18 P. T. Beurskens, G. Admiraal, G. Beurskens, W. P. Bosman, R. de Gelder, R. Israel and J. M. M. Smits, The DIRDIF-94
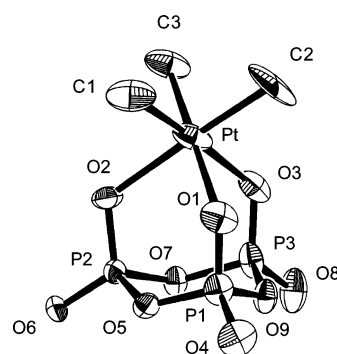
Fig. 4 Experimental (left) and computed (right) ^{31}P–{^{1}H} NMR spectra of **6**.

Fig. 5 Eyring plot of the temperature dependence of the rate constants (*k*) for the intramolecular ligand exchange in **6**.

(Fig. 5) gives the activation parameters $\Delta H^{\ddagger} = 45 \pm 1$ kJ mol^{-1}, $\Delta S^{\ddagger} = 10 \pm 6$ J mol^{-1} K^{-1} and $\Delta G^{\ddagger} = 42 \pm 2$ kJ mol^{-1} (−40 °C). The relatively small but positive $\Delta S^{\ddagger}$ value is compatible with the above-mentioned intramolecular associative mechanism where the pseudo-rotation–chelate inversion is the rate-determining process (Scheme 4).

Synthesis and structure of (PPN)$_2$[PtMe$_3$(P$_3$O$_9$)] (7)

Finally, the synthesis and structure of the Pt(IV) P$_3$O$_9$ complex (PPN)$_2$[PtMe$_3$(P$_3$O$_9$)] (**7**) was investigated. This complex was prepared by the reaction of [PtMe$_3$I]$_4$ with (PPN)$_3$(P$_3$O$_9$) in CH$_2$Cl$_2$ at room temperature and isolated as stable colorless crystals. Both ^{31}P–{^{1}H} and ^{1}H NMR spectra exhibit one singlet for the P$_3$O$_9$ ligand [δ −9.3, ^{2}J(PtP) 63 Hz] and the Me groups (δ 1.02), respectively, indicating a C_{3v} molecular symmetry for this anion.

The molecular structure of **7** has been unambiguously determined by X-ray diffraction study (Fig. 6 and Table 3). The platinum centre adopts a typical octahedral geometry, where the Pt–O distances [2.20 Å (mean)] are slightly longer than those found in complexes **3**–**6**. Similar κ^3-coordination of the P$_3$O$_9$ ligand has been commonly found in d^6-metal complexes.[5a,b,f,7a,8] The O(8) atom in the P$_3$O$_9$ ligand in **7** is located in the vicinity of the C(66)–H(61) group of a PPN

program system, Technical Report of the Crystallography Laboratory, University of Nijmegen, The Netherlands, 1994.

19 P. T. Beurskens, G. Admiraal, G. Beurskens, W. P. Bosman, R. de Gelder, R. Israel and J. M. M. Smits, The DIRDIF-99 program system, Technical Report of the Crystallography Laboratory, University of Nijmegen, The Netherlands, 1999.

20 F. R. Hartley, S. G. Murray and A. Wilkinson, *Inorg. Chem.*, 1989, **28**, 549.

21 J.-F. Ma, Y. Kojima and Y. Yamamoto, *J. Organomet. Chem.*, 2000, **616**, 149.

22 G. R. Desiraju and T. Steiner, *The Weak Hydrogen Bond in Structural Chemistry and Biology*, Oxford University Press, New York, 2001.

23 T. Rüther, M. C. Done, K. J. Cavell, E. J. Peacock, B. W. Skelton and A. H. White, *Organometallics*, 2001, **20**, 5522.

24 J. A. Casares, P. Espinet, J. M. Martínez-Ilarduya and Y.-S. Lin, *Organometallics*, 1997, **16**, 770.

25 K. Ohta, M. Hashimoto, Y. Takahashi, S. Hikichi, M. Akita and Y. Moro-oka, *Organometallics*, 1999, **18**, 3234; M. Akita, M. Hashimoto, S. Hikichi and Y. Moro-oka, *Organometallics*, 2000, **19**, 3744.

26 C. K. Johnson, ORTEP, Report ORNL-5138, Oak Ridge National Laboratory, Oak Ridge, TN, USA, 1976.

27 V. D. Makhaev, Z. M. Dzhabieva, S. V. Konovalikhin, O. A. D'yachenko and G. P. Belov, *Russ. J. Coord. Chem.*, 1996, **22**, 563.